1380, 1335, 1240, 1210, 1140, 1110 (s), 1060, 1015, 1005 cm^{-1}; ^1H NMR (250 MHz, $CDCl_3/D_2O$) δ 7.35 (m, 5 H, C_6H_5), 4.68 and 4.38 (2d, J = 11.3, 11.3, 2 H, CH_2Ph), 4.15 (m, 1 H, $COCHCH_3$), 4.06 and 4.00 (2d, J = 8.0, 8.0, 2 H, CHN, $CHOC{=}O$), 3.85 (dd, J = 7.5, 4.9, 1 H, $CHOD$), 3.48 (m, 1 H, $CHOCH_2Ph$), 2.20 (d, J = 4.5, 1 H, C-7 H), 1.85-1.08 (m, 4 H, C-8 and C-9 H), 1.30 [d, J = 7.1, 3 H, $CH(CH_3)O$], 1.15 (d, J = 7.1, 3 H, $COCHCH_3$), 1.03 (s, 3 H, C-1 CH_3), 0.96 and 0.88 (2s, 6 H, C-10 CH_3). CI MS: m/e 416.2422 $(M + H)^+$. Calcd for $C_{24}H_{34}NO_5$: m/e 416.2437.

(2*R*,3*R*,4*S*)-4-(Benzyloxy)-3-hydroxy-2-methylpentanoic Acid (13g): colorless oil; IR (CH_2Cl_2) 3580 (br), 3490 (br), 3080, 3030, 2975, 2940, 2890, 1705, 1605, 1495, 1460, 1380, 1140, 1110 (s), 1080, 1035 cm^{-1}; ^1H NMR (250 MHz, $CDCl_3/D_2O$) δ 7.32 (m, 5 H, C_6H_5), 4.63 and 4.43 (2d, J = 11.5, 11.5, 2 H, CH_2Ph), 3.94 (dd, J = 6.4, 5.0, 1 H, $CHOD$), 3.51 (m, 1 H, $CHOCH_2Ph$), 2.82 (qd, J = 7.1, 5.0, 1 H, $COCHCH_3$), 1.28 [d, J = 6.2, 3 H, $CH(CH_3)O$], 1.20 (d, J = 7.1, 3 H, $COCHCH_3$). CI MS: m/e 239.1253 $(M + H)^+$. Calcd for $C_{13}H_{19}O_4$: m/e 239.1283.

***N*-[(2*S*,3*S*,4*S*)-4-(Benzyloxy)-3-hydroxy-2-methylpentanoyl]-(1*R*,2*S*,6*R*,7*S*)-1,10,10-trimethyl-4-oxo-5-aza-3-oxatricyclo[5.2.1.0^{2,6}]-decane (19)**: mp 75-76 °C (after recrystallization); ^1H NMR (250 MHz, $CDCl_3$) δ 7.38 (m, 5 H, C_6H_5), 4.67 and 4.47 (2d, J = 11.3, 11.3, 2 H, CH_2Ph), 4.33 and 4.29 (2d, J = 8.2, 8.1, 2 H, CHN, $CHOC{=}O$), 4.03 (m, 1 H, $COCHCH_3$), 3.85 (dd, J = 6.2, 4.6, 1 H, $CHOD$), 3.58 (m, 1 H, $CHOCH_2Ph$), 2.24 (d, J = 4.5, 1 H, C-7 H), 1.6-1.1 (m, 4 H, C-8 and C-9 H), 1.28 [d, J = 6.2, 3 H, $CH(CH_3)O$], 1.17 (d, J = 6.91, 3 H, $COCHCH_3$), 1.05 (s, 3 H, C-1 CH_3), 0.97 and 0.86 (2s, 6 H, C-10 CH_3). CI MS: m/e 416.2496 $(M + H)^+$. Calcd for $C_{24}H_{34}NO_5$: m/e 416.2437.

***N*-[(2*R*,3*R*,4*R*)-3-Acetoxy-4-(benzyloxy)-2-methylpentanoyl]-(1*R*,2*S*,6*R*,7*S*)-1,10,10-trimethyl-4-oxo-5-aza-3-oxatricyclo[5.2.1.0^{2,6}]-decane (20)**: colorless oil; IR (CH_2Cl_2) 2950, 2875, 1760(s), 1735, 1685, 1480, 1450, 1375, 1360, 1330, 1240, 1210, 1060, 1010, 1000 cm^{-1}; ^1H NMR (250 MHz, $CDCl_3$) δ 7.32 (m, 5 H, C_6H_5), 5.44 (dd, J = 8.1, 6.9, 1 H, $CHOAc$), 4.61 and 4.38 (2d, J = 11.3, 11.3, 2 H, CH_2Ph), 4.18 (m, 1 H, $COCHCH_3$), 3.78 and 3.67 (2d, J = 7.9, 7.9, 2 H, CHN, $CHOC{=}O$), 3.55 (m, 1 H, $CHOCH_2Ph$), 2.15 (d, J = 4.4, 1 H, C-7 H), 2.10 (s, 3 H, $COCH_3$), 1.75-1.40 (m, 4 H, C-8 and C-9 H), 1.20 (d, J = 6.2, 3 H, $CHCH_3OCH_2Ph$), 1.10 (d, J = 6.9, 3 H, $COCHCH_3$), 0.99 (s, 3 H, C-1 CH_3), 0.91 and 0.84 (2s, 6 H, C-10 CH_3). CI MS: m/e 458.2533 $(M + H)^+$. Calcd for $C_{26}H_{36}NO_6$: m/e 458.2542.

***N*-[(*Z*)-1-[(*tert*-Butyldimethylsilyl)oxy]-1-propenyl]-(1*R*,2*S*,6*R*,7*S*)-1,10,10-trimethyl-4-oxo-5-aza-3-oxatricyclo[5.2.1.0^{2,6}]-decane (21)**. To diisopropylamine (175 μL, 1.25 mmol) in THF (2.0 mL) was added n-butyllithium solution in hexanes (1.23 M, 1.02 mL, 1.25 mmol) dropwise at 0 °C (ice bath). After stirring for 15 min, the solution was cooled to -78 °C (dry ice-acetone bath), N-propionyloxazolidinone **6** (286 mg, 1.14 mmol) in THF (2.0 mL) was added dropwise over 5 min, and the reaction mixture was stirred for 1 h at -78 °C. A solution of *tert*-butyldimethylsilyl trifluoromethanesulfonate (265 μL, 1.14 mmol) was then added dropwise over 2 min. The dry ice-acetone bath was removed, and the solution was allowed to warm to ca. 25 °C over 1 h. A solution of pH 7 phosphate buffer (2.0 mL) was added, and the mixture was extracted twice with ether (100 mL each). The ether layers were dried ($MgSO_4$), vacuum-filtered, concentrated by rotary evaporation, and placed under high vacuum (ca. 0.1 mmHg) for 2 h to yield an off-white solid, **21**: mp 110-111 °C (348 mg, 84%); was purified by flash chromatography (9:1, petroleum ether-diethyl ether), R_f = 0.19; $[\alpha]^{24}_D$ +37° (c 0.75, CH_2Cl_2); IR ($CHCl_3$) 2990, 2950, 2875, 2850, 1745 (s), 1690, 1470, 1465, 1420, 1350, 1340, 1260, 1150, 1120, 1060 cm^{-1}; ^1H NMR (250 MHz, $CDCl_3$) δ 4.60 (q, J = 6.9, 1 H, $C{=}CHCH_3$), 4.08 and 3.75 (2d, J = 8.2, 8.2, 2 H, CHN, $CHOC{=}O$), 1.85 (d, J = 4.5, 1 H, C-7 H), 1.48 (d, J = 6.9, 3 H, $C{=}CHCH_3$), 1.7-0.8 (m, 4 H, C-8 and C-9 H), 0.88 (s, 6 H, C-10 CH_3), 0.81 (s, 9 H, *tert*-butyl H), 0.74 (s, 3 H, C-1 CH_3), 0.044 and 0.00 (2s, 6 H, CH_3Si). CI MS: m/e 366.2459 $(M + H)^+$. Calcd for $C_{20}H_{36}NO_3Si$: m/e 366.2464.

Acknowledgment. We thank Dr. Patrick Carroll, X-ray Diffraction Facility, Dr. George Furst, NMR Facility, and Dr. John Dykins, Mass Spectrometry Facility, for their splendid assistance, and Dr. D. R. Reddy of this laboratory for sharing his observations on selective reactions of camphorquinone. We gratefully acknowledge support by the University of Pennsylvania Research Fund and by the National Institutes of Health.

Supplementary Material Available: Tables of refined atomic positional and thermal parameters for the five X-ray structures reported and ORTEP diagrams for compounds **7**, **9**, **18**, **19**, and **21** (47 pages). Ordering information is given on any current masthead page.

An Electron Donor-Acceptor Complex and a Thermal Triplex as Intermediates in the Cycloaddition Reaction of *N*-Vinylcarbazole with Dimethyl 2,2-Dicyanoethylene-1,1-dicarboxylate

Tetsuya Gotoh, Anne Buyle Padias, and H. K. Hall, Jr.*

Contribution from C. S. Marvel Laboratories, Department of Chemistry, The University of Arizona, Tucson, Arizona 85721. *Received May 21, 1990*

Abstract: The formation of dimethyl 1-(carbazol-9-yl)-2,2-dicyanocyclobutane-3,3-dicarboxylate through a tetramethylene zwitterionic intermediate (T) by the reaction of *N*-vinylcarbazole (NVCZ) and dimethyl 2,2-dicyanoethylene-1,1-dicarboxylate in nonpolar and moderately polar solvents was studied kinetically. Two competitive formation paths of T were found: (a) unimolecular transformations of the electron donor-acceptor (EDA) complex and (b) bimolecular reaction between the EDA complex and free NVCZ. Contributions of these two reactions to the overall reaction are influenced by the solvent and the concentration of NVCZ. The third-order kinetics is explained on the basis that the contribution of the cation-radical form to the transition state can be enhanced by an additional donor molecule through charge resonance in a thermal triplex. This may be a general mode of catalysis for reactions of electron-rich unsaturated molecules with electrophiles.

Introduction

Even though the reactions of electrophilic olefins with nucleophilic olefins have been studied by many investigators, detailed kinetic studies have been rather infrequent. Huisgen studied in detail the reaction of vinyl ethers and of vinyl sulfides with tetracyanoethylene (TCNE).[1] The reactions were reported to follow second-order kinetics in all cases. Although electron donor-acceptor (EDA) complexes were observed in these reactions, the question of their participation in the cycloaddition reactions was left open. In Bartlett's review,[2] the cycloaddition of *p*-meth-

(1) Huisgen, R. *Acc. Chem. Res.* **1977**, *10*, 117.

0002-7863/91/1513-1308$02.50/0

Scheme I. Reaction Mechanism

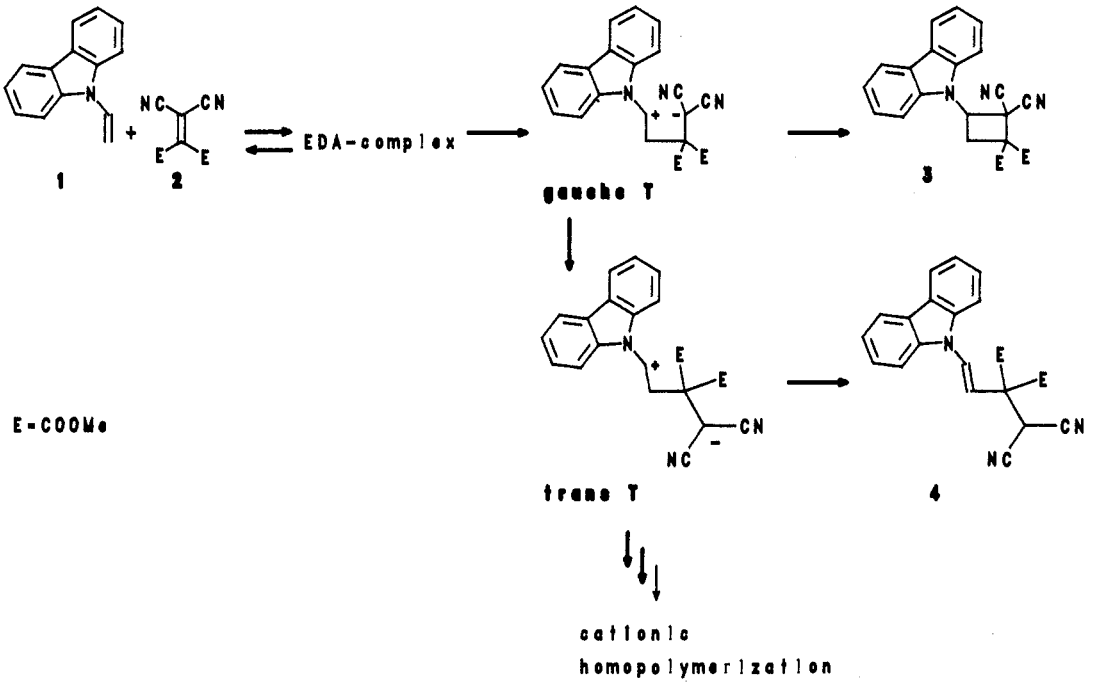

oxystyrene to TCNE is described and here again the rate constants were second order. No correlation between EDA complexing abilities and cycloaddition constants was found.

The question of whether or not the EDA complex lies on the reaction path is fundamental to our understanding of the cycloaddition reaction mechanism. This question has been discussed several times previously. A negative enthalpy of activation allowed Kiselev and Miller to conclude that the EDA complex was an intermediate in the Diels–Alder reaction of TCNE with 9,10-dimethylanthracene.[3] However, Huisgen noted that this criterion does not apply to [2 + 2] cycloadditions.[1]

Other important related studies of the reaction of an electron-rich unsaturated molecule with electrophiles have dealt with aromatic substitution reactions. *N,N*-Dimethylaniline (DMA) reacts with TCNE to yield first the tetracyanoethane and later the tricyanoethene derivative.[4-6] Strong EDA complexes were seen. The reaction kinetics showed a second-order term in the donor molecule DMA, and a primary kinetic isotope effect was observed.

Subsequently, Kochi generalized this work and placed the EDA complex on the reaction path in reactions of both olefins and aromatic compounds with electrophiles.[7]

Earlier, as part of a comprehensive study of this field,[8] we studied the reactions of the very electron-rich *N*-vinylcarbazole (NVCZ, **1**) with electrophilic tetrasubstituted ethylenes.[9] Although the cycloaddition reaction was reversible to components in the case of TNCE, the reaction of slightly less electrophilic dimethyl 2,2-dicyanoethylene-1,1-dicarboxylate (DDED, **2**) with **1** was not reversible and the charge-transfer color of the component mixture disappeared completely. The complete course of reaction is shown in Scheme I. Dimethyl 1-(carbazol-9-yl)-2,2-dicyanocyclobutane-3,3-dicarboxylate (**3**) was formed as the primary product in a rapid step. The thermodynamically favored product is *trans*-dimethyl 1-(carbazol-9-yl)-4,4-dicyano-1-butene-3,3-dicarboxylate (**4**), but we have not studied this phase of the reaction kinetically. The existence of the zwitterionic tetramethylene intermediate T has been proven by use of stereochemical evidence and trapping experiments. Evidence for the existence of both gauche-T and trans-T was found. No evidence for electron-transfer, such as cyclic dimer of NVCZ, was found, and the kinetics were consistent with the tetramethylene zwitterion as the key intermediate. This is in contrast to some recent literature concerning the Diels–Alder cycloaddition of the extremely electron-rich diene tetrakis(dimethylamino)-1,2-dimethylenecyclohexane with TCNE in which evidence for electron transfer was found.[10]

The present in-depth study of cyclobutane formation in the *N*-vinylcarbazole (NVCZ, **1**)/dimethyl 2,2-dicyanoethylene-1,1-dicarboxylate (DDED, **2**) system was undertaken to elucidate the role of the EDA complex in this reaction and to look for possible kinetic terms larger than first order in donor NVCZ.

Results

Equilibrium of Electron Donor–Acceptor Complex Formation. An intense red color due to the EDA complex (λ_{EDA}^{max} = 430–458 nm, depending on the solvent) is formed upon mixing solutions of the reactants **1** and **2**. If the EDA complex is 1:1 with respect to donor **1** and acceptor **2**, the following relations are valid under initial conditions before significant reaction has occurred

$$K_{EDA} = \frac{[EDA]_{t=0}}{[D]_0[A]_{t=0}} \quad (1)$$

and

$$[A]_0 = [A]_{t=0} + [EDA]_{t=0} \quad (2)$$

where $[A]_0$ and $[D]_0$ denote the concentrations of acceptor **2** and donor **1** in the feed, $[EDA]_{t=0}$ and $[A]_{t=0}$ denote the initial concentrations of EDA complex and acceptor, and K_{EDA} denotes the formation constant of the EDA complex. Thus

$$[EDA]_{t=0} = \frac{K_{EDA}[D]_0}{1 + K_{EDA}[D]_0}[A]_0 \quad (3)$$

and

$$OD_{t=0} = \epsilon_{EDA}[EDA]_{t=0}l \quad (4)$$

(2) Bartlett, P. D. *Q. Rev., Chem. Soc.* **1970**, *24*, 473.
(3) Kiselev, V. D.; Miller, J. G. *J. Am. Chem. Soc.* **1975**, *97*, 4036.
(4) Rappoport, Z. *J. Chem. Soc.* **1963**, 4498.
(5) Garbutt, S.; Gerrard, D. L. *J. Chem. Soc., Perkin Trans. 2* **1972**, 782.
(6) Nogami, T.; Nakano, Y.; Hasegawa, Y.; Shirota, Y.; Mikawa, H. *Bull. Chem. Soc. Jpn.* **1979**, *52*, 2110.
(7) Kochi, J. K. *Angew. Chem., Int. Ed. Engl.* **1988**, *27*, 1227 and references therein.
(8) Hall, H. K., Jr.; Padias, A. B. *Acc. Chem. Res.* **1990**, *23*, 3 and references therein.
(9) Gotoh, T.; Padias, A. B.; Hall, H. K., Jr. *J. Am. Chem. Soc.* **1986**, *108*, 4920.
(10) Sustmann, R.; Necking, K.; Kopp, G.; Rose, M. *Angew. Chem., Int. Ed. Engl.* **1989**, *28*, 1713.

Table I. Formation Constants of EDA Complex and Related Spectroscopic and Thermodynamic Parameters

solvent	λ_{max} (nm)	ϵ_{max} (L mol^{-1} cm^{-1})	K_{EDA} (L mol^{-1}) (T (°C))			ΔH_{EDA} (kJ mol^{-1})	ΔS_{EDA} (J K^{-1} mol^{-1})	ΔG_{EDA} (25 °C) (kJ mol^{-1})
CH_2Cl_2	438	600 ± 20	0.202 (20)	0.192 (25)	0.182 (30)	−8.5	−42	4.1
$CHCl_3$	458	4530 ± 150	0.0311 (15)	0.0299 (20)	0.0284 (30)	−7.7	−55	8.7
CCl_4	430	910 ± 30	0.259 (40)	0.252 (45)	0.243 (50)	−6.1	−31	3.1
C_6H_6	430	1030 ± 40	0.142 (30)	0.133 (40)	0.120 (50)	−7.6	−41	4.6

Table II. Rate Constants k_2 and k_3

solvent	10^2k_2 (s^{-1}) (T (°C))			10^2k_3 (L mol^{-1} s^{-1}) (T (°C))		
CCl_4	0.238 (40)	0.331 (45)	0.428 (50)	1.00 (40)	1.25 (45)	1.47 (50)
CH_2Cl_2	2.39 (20)	3.08 (25)	3.90 (30)	0.97 (20)	1.46 (25)	2.13 (30)
C_6H_6	1.00 (30)	1.45 (40)	2.00 (50)	1.17 (30)	2.26 (40)	3.67 (50)
$CHCl_3$	15.7 (15)	19.7 (20)	24.2 (25)	5.80 (15)	6.80 (20)	8.00 (25)

where l is the optical path length, $OD_{t=0}$ the absorbance of the EDA complex, and ϵ_{EDA} the molar extinction coefficient of the EDA complex. The plots in Figure 1 show the linearity of the relationship of the initial absorbance of the EDA complex both vs the factor containing $[D]_0$ and vs the acceptor concentration in the feed $[A]_0$. The 1:1 stoichiometry of the EDA complex is thus confirmed in the solvents used in this study.

The Benesi–Hildebrand method[11] was applied to determine the formation constant of the EDA complex (K_{EDA}) and the molar extinction coefficient (ϵ_{EDA}). The following relationship was used:

$$\frac{[A]_0 l}{OD_{t=0}} = \frac{1}{K_{EDA}\epsilon_{EDA}} \frac{1}{[D]_0} + \frac{1}{\epsilon_{EDA}} \tag{5}$$

Linear plots of $[A]_0/OD$ vs $1/[D]_0$ were obtained over a range of $[D]_0$ (0.4–1.2 M) at several temperatures. The values of the equilibrium constant K_{EDA} obtained in several solvents are summarized in Table I. The thermodynamic parameters for EDA complexation, ΔG_{EDA}, ΔH_{EDA}, and ΔS_{EDA}, were obtained from the following thermodynamic relations

$$\frac{\delta \ln K_{EDA}}{\delta(1/T)_p} = -\frac{\Delta H_{EDA}}{R} - \alpha T^2 \tag{6}$$

$$\Delta S_{EDA} = \frac{\Delta H_{EDA} + RT \ln K_{EDA}}{T} \tag{7}$$

where α is the expansion coefficient of the solvent.[12] The negative values of ΔH_{EDA} and ΔS_{EDA}, also given in Table I, are not large; i.e., the complex is weak.

Kinetics Scheme. The following kinetic scheme will be proposed:

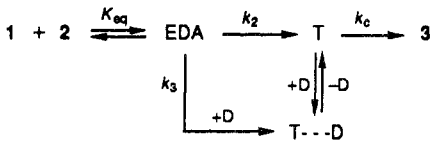

As we shall see, the tetramethylene T can be formed through unimolecular collapse of the EDA complex (k_2 process) or by bimolecular reaction of the EDA complex with free donor (k_3 process). The k_2 process is first order in both donor and acceptor concentration, while the k_3 process is second order in donor concentration and first order in acceptor concentration. The rate constant k_c represents the cyclization rate constant. In the reaction conditions used, this last step is irreversible.

Kinetics–Mathematical Treatment of Disappearance of EDA Complex. All measurements in this study were performed under pseudo-first-order reaction conditions, using a large excess of **1** (at least 20 times). By use of $[D]_0 \gg [A]_0$, the following equations can be written

$$d[\mathbf{3}]/dt = k_c[T] \tag{8}$$

$$d[T]/dt = k_2[EDA] + k_3[EDA][D]_0 - k_c[T] \tag{9}$$

$$K_{EDA} = [EDA]/[D]_0[A] \tag{10}$$

$$[A]_0 = [A] + [EDA] + [\mathbf{3}] + [T] \tag{11}$$

where [ ] expresses the concentration at any time t and [ ]$_0$ is the initial concentration. The steady-state approximation

$$d[T]/dt = 0 \tag{12}$$

is used. The equations above lead to the following expression for the disappearance of EDA complex

$$[EDA] = [EDA]_{t=0} \exp(-k_{obsd}t) \tag{13}$$

$$k_{obsd} = (k_2 + k_3[D]_0)\frac{K_{EDA}[D]_0}{1 + K_{EDA}[D]_0} \tag{14}$$

where k_{obsd} denotes the pseudo-first-order rate constant for the disappearance of EDA complex. By plotting ln OD vs time, a linear plot is obtained: the slope corresponds to $-k_{obsd}$ and the intercept ln $(\epsilon_{EDA}[EDA]_{t=0}l)$.

The values thus obtained with varying $[D]_0$ were plotted as k_{obsd} $((1 + K_{EDA}[D]_0)/K_{EDA}[D]_0)$ vs $[D]_0$. The plots in Figure 2 showed good linear behavior with the slope equal to k_3 (the second-order rate constant for the bimolecular reaction between EDA complex and free donor) and the intercept k_2 (the first-order rate constant for the unimolecular transformation of EDA complex). The values obtained for k_2 and k_3 with varying temperature and solvent are

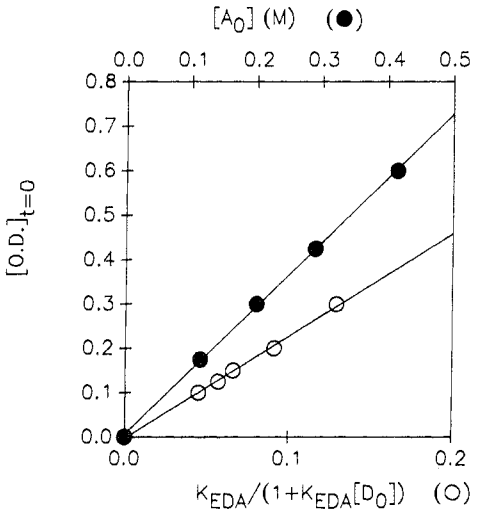

Figure 1. 1:1 stoichiometry in EDA complex formation in the DDED–NVCZ system in benzene at 50 °C.

(11) Benesi, H. A.; Hildebrand, J. H. *J. Am. Chem. Soc.* **1949**, *71*, 2703.
(12) Riddick, J. A.; Bunger, W. B. Organic Solvents. In *Techniques of Chemistry*, 3rd ed.; Weissberger, A., Ed.; Wiley-Interscience: New York, 1970.

Table III. Activation Parameters for k_2 and k_3

solvent	$\Delta H^{\ddagger}_2$ (kJ mol^{-1})	$\Delta S^{\ddagger}$ (J K^{-1} mol^{-1})	$\Delta G^{\ddagger}_2$ (25 °C) (kJ mol^{-1})	$\Delta H^{\ddagger}_3$ (kJ mol^{-1})	$\Delta S^{\ddagger}_3$ (J K^{-1} mol^{-1})	$\Delta G^{\ddagger}_3$ (25 °C) (kJ mol^{-1})
CH_2Cl_2	34.0	−160	82.5	55.8	−93	84.0
$CHCl_3$	28.1	−163	76.6	20.3	−198	79.3
CCl_4	46.9	−146	90.4	30.3	−187	86.1
C_6H_6	25.3	−200	84.9	43.8	−138	84.8

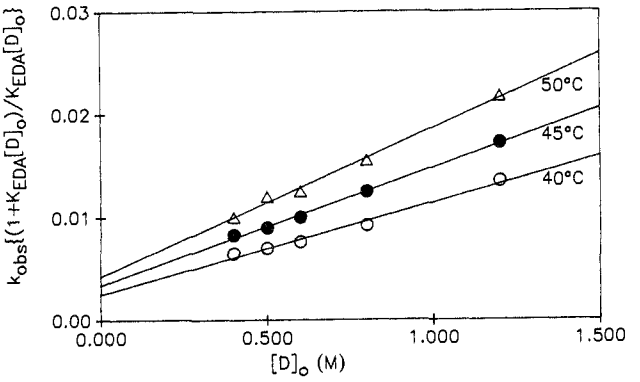

Figure 2. Dependence of the rates on donor concentration: $[A]_0 = 2.07 \times 10^{-2}$ M.

summarized in Table II. Both k_2 and k_3 processes are responsible for the formation of T. The contribution of the k_3 process is particularly significant at high donor concentrations.

Activation Parameters. Activation parameters for k_2 and k_3 processes are obtained from the Eyring equation

$$R \ln \frac{hk_i}{k_B T} = -\frac{\Delta G_i^{\ddagger}}{T} = -\frac{\Delta H_i^{\ddagger}}{T} + \Delta S_i^{\ddagger} \qquad (15)$$

where h, k_B, and k_i are the Planck constant, the Boltzmann constant, and the rate constant (k_2 and k_3), respectively, and are listed in Table III. Fairly large negative entropies demonstrate that the transition states require very strict configurations.

Linear Free Energy Relationships between ΔG_{EDA} and $\Delta G^{\ddagger}$ for Both the k_2 and the k_3 Processes. For the k_3 process, linear plots of $\Delta G_3^{\ddagger}$ and $(\Delta G_3^{\ddagger} + \Delta G_{EDA})$, which correspond to the activation free energy for the entire formation process of T through bimolecular reaction of EDA complex and free donor, against ΔG_{EDA} are shown in Figure 3. For the k_2 process, similar linear correlations were found for the plots of $\Delta G_2^{\ddagger}$ and $(\Delta G_2^{\ddagger} + \Delta G_{EDA})$ against ΔG_{EDA} (Figure 4).

Absence of "Medium Effect". We interpreted our data in terms of coexistence of k_2 and k_3 processes for the formation of T. One may be suspicious about this conclusion by taking the medium effect into account caused by the use of high donor concentration. However, we can exclude this possibility as follows. The medium effect may be expressed as

$$k_{obsd} = k_2(1 + \alpha[D]_0)\frac{K_{EDA}[D]_0}{1 + K_{EDA}[D]_0} \qquad (16)$$

where α denotes the medium effect coefficient for the donor concentration change. Then, k_3 in eq 14 would correspond to αk_2 in eq 16. If this were the case, k_3 should have the same activation parameters as k_2. As clearly seen in Table III, k_2 and k_3 have characteristic, different activation parameters. The result shows that k_2 and k_3 processes are independent of each other. Next, we point out that K_{EDA}, which is very sensitive to the environmental change as is evidenced by solvent effect in Table I, is obtained from the excellent linear relationship in the Benesi–Hildebrand plot, even in carbon tetrachloride in which the largest contribution of k_3 process is observed. We take this as evidence against the medium effect as an explanation.

Discussion

Evidence That the EDA Complex Is on the Reaction Path. From our results, two different processes compete in the formation of the tetramethylene T: the k_2 process, which is first order in EDA complex concentration, and the k_3 process, which corresponds to a bimolecular reaction of donor and EDA complex.

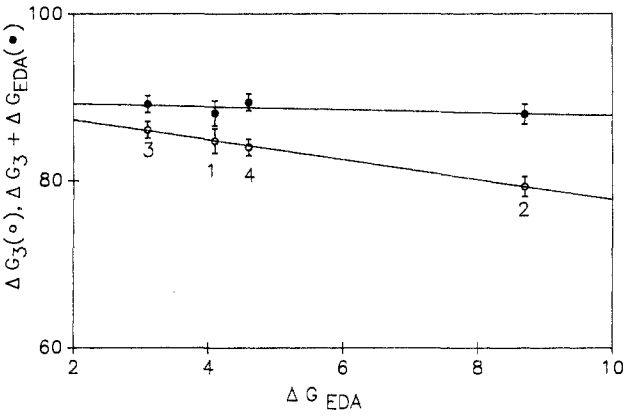

Figure 3. Linear free energy relationships between rates (k_3) and EDA equilibrium constants: 1, in dichloromethane; 2, in chloroform; 3, in carbon tetrachloride; 4, in benzene.

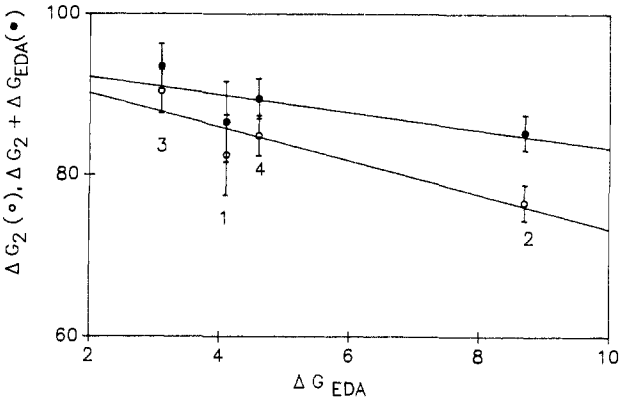

Figure 4. Linear free energy relationships between rates (k_2) and EDA equilibrium constants: 1, in dichloromethane; 2, in chloroform; 3, in carbon tetrachloride; 4, in benzene.

Linear relationships were found between the activation free energies of the composite processes. The k_3 process undoubtedly involves EDA complex on the reaction path. This conclusion is supported by considering the additivity of the activation free energy shown in Figure 3. From the linearity between $\Delta G_3^{\ddagger}$ and ΔG_{EDA}, we can conclude that the same factors govern both EDA complexation and bimolecular reaction between EDA complex and free donor. The negative sign of the slope shows that interactions between solvent and free donor–acceptor system and between solvent and the transition state are much alike and are stronger than those between solvent and EDA complex.

A linear relationship is also found in the plot of $(\Delta G_2^{\ddagger} + \Delta G_{EDA})$ vs ΔG_{EDA} (Figure 4). This suggests that the EDA complex is also a true intermediate in the k_2 process. Formation of T through the transformation of EDA complex occurs through the bimolecular reaction of free donor and acceptor, since the same correlations between $\Delta G^{\ddagger}$ and ΔG_{EDA} for k_2 and k_3 processes are not expected if EDA complexation is merely a side reaction of the k_2 process.

Proposed Mechanism. It is well-known that cation radicals of donor molecules readily complex with the parent molecule. For

Scheme II

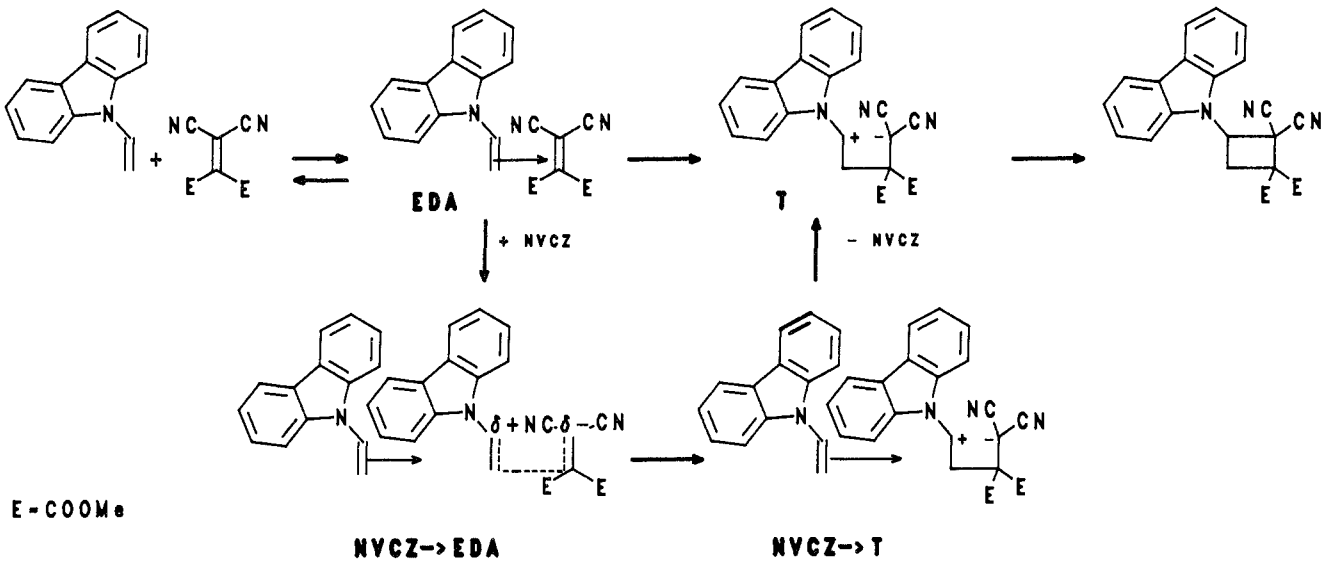

example, the cation radical of NVCZ forms a complex with NVCZ.[13]

$$\text{NVCZ} \xrightarrow{h\nu} \text{NVCZ}^{\bullet+} \xrightarrow{\text{NVCZ}} \underset{\substack{\text{dimer}\\\text{radical cation}}}{(\text{NVCZ})_2^{\bullet+}}$$

This interaction is particularly effective in that dimeric cation radicals are heavily stabilized by charge resonance between two structures of equal energy and the ideal symmetry.

$$\text{NVCZ} \rightarrow \text{NVCZ}^{\bullet+} \leftrightarrow {}^{+\bullet}\text{NVCZ} \leftarrow \text{NVCZ}$$

This can be viewed as a new CT complex between D (donor) and $D^{\bullet+}$ (acceptor). Alternatively, the second donor molecule can be viewed as a uniquely specific solvating molecule.

Schanne and Staab demonstrated this effect in rigid complexes of paracyclophanes with TCNE.[13] The donor ability of a dimethoxyphenyl ring is increased by the other parallel ring of the paracyclophane, if the latter also has donor substituents. This is shown by a shift of the λ_{max} of the charge-transfer complex with TCNE to longer wavelengths and by a lowering of the ionization potential.

On the basis of these literature data and our results, we propose that the k_2 process proceeds via direct collapse of the EDA complex, while in the k_3 process the second NVCZ molecule stabilizes the donor moiety of the EDA complex and this leads to zwitterion complexed with donor (Scheme II).

Relationship to Photochemical Triplex Reaction. Exciplexes are involved in photochemical donor–acceptor reactions as charge-transfer complexes are involved in thermal reactions. The overwhelming majority of exciplex reactions are first order. Apparently, the only examples of bimolecular reaction of an exciplex with another organic molecule are described recently by Schuster[15,16] in the reaction of indene (In) and a diene in the presence of dicyanoanthracene, for which the following mechanism was proposed:

$$\text{In} \xrightarrow{h\nu} \underset{\substack{\text{excited}\\\text{singlet}}}{\text{In}^{1}*} + \text{DCA} \rightarrow \underset{\substack{\text{polar singlet}\\\text{exciplex}}}{\text{In}\cdot\text{DCA}^{1}*} + \text{diene} \rightarrow$$

$$\underset{\substack{\text{polar singlet}\\\text{triplex}}}{\text{diene–In–DCA}^{1}*} \rightarrow \text{cycloadducts} + \text{DCA}$$

The diene can stabilize the increasingly positive indene fragment by charge-resonance interaction. Because in this case the acceptor molecule is aromatic, the two olefinic donor molecules react to form the observed cycloadducts.

Relationship to Rappoport Work. The kinetics of our cycloaddition reaction are the same as those of the aromatic substitution reaction studied by Rappoport and others[4-6] in that a second donor amine molecule plays an important role. However, the key observation of a primary kinetic isotope effect by Shirota and coworkers[6] implies that the second molecule acts as a base, transferring the proton or deuteron in the rate-determining step.

Conclusion

A second donor molecule has been shown to catalyze tetramethylene formation in a [2 + 2] cycloaddition. Along with the results of Schuster,[15,16] these results suggest new possibilities in the specific molecular catalysis of both thermal and photochemical reactions of unsaturated molecules. It is interesting to note that Woodward envisaged this possibility almost 50 years ago.[17]

Experimental Section

Detailed description of the experiments already appeared in the preceding paper.[9] Solvents were purified as described.[12] Temperature of the thermostated water was kept constant to ±0.05 °C. Quartz cells of 1-cm optical path length were used.

For determining the variation of rate constants with temperature, we were restricted to the rather narrow range of 10–20 °C. The high concentrations required for donor NVCZ determined the lower limits of temperature range because of NVCZ solubility. The higher limits of the temperature range were determined by the volatility of the solvents used, especially at the altitude (800 m) of our laboratory. In benzene, the temperature range was 20 °C because of lower volatility.

The reliability of Eyring parameters (Table III) calculated from k_2 and k_3 at three different temperatures over this rather narrow temperature range depends on reproducibilities and deviations between measured k_2 and k_3 values. The k_2 and k_3 values were obtained from the plots like Figure 2. In this kind of figure, each data point for k_{obsd} was derived by averaging values from at least six independent measurements. Reproducibility for k_{obsd} was good and deviations between each value from independent measurements were small, less than ±1%. The deviations for k_2 and k_3 values from such plots were estimated to be within ±2% for k_2 and within ±1% for k_3. Consequently, Eyring parameters should reflect those k_2 and k_3 deviations in their accuracy and were estimated to be less than ±6% in the worst case for $\Delta G_2^{\ddagger}$.

Acknowledgment. We are deeply indebted to the National Science Foundation, Division of Materials Research, for financial support of this work.

Registry No. 1, 1484-13-5; **2**, 82849-49-8.

(13) Ledwidth, A. *Acc. Chem. Res.* **1972**, *5*, 133.
(14) Schanne, L.; Staab. H. A. *Tetrahedron Lett.* **1984**, *25*, 16.
(15) Calhoun, G. C.; Schuster, G. B. *J. Am. Chem. Soc.* **1986**, *108*, 8021.
(16) Akbulut, N.; Hartsough, D.; Kim, J.-I.; Schuster, G. B. *J. Org. Chem.* **1989**, *54*, 2549.
(17) Woodward, R. B. *J. Am. Chem. Soc.* **1942**, *64*, 3058. "...the possibility of catalysis by donor or acceptor molecules which cannot themselves participate in the diene-addition reaction. Preliminary experiments designed to test this possibility gave some qualitative indication that dimethylaniline and 1,3,5-trinitrobenzene exert such an accelerating effect."